Ballast Settlement Ramp to Mitigate Differential Settlement in a Bridge Transition Zone

Yu Qian, Erol Tutumluer, Youssef M. A. Hashash, Jamshid Ghaboussi, and David D. Davis

Differential settlement in railroad track transitions, often associated with differences in track stiffness, may apply considerable impact load and may cause rapid deterioration of track geometry. Such differential settlement commonly seen in bridge approaches may lead to problems in ride comfort, track safety, and reliability. Ballast and subballast layers have been identified as a major cause of differential settlement related to the particulate nature of the aggregate deformation behavior causing degradation and breakdown associated with increased track usage. This paper describes an innovative field approach that successfully demonstrated the use of engineered ballast materials for reducing or mitigating the differential settlement problem in a bridge transition zone. Discrete element method (DEM) simulations were used to predict full-scale track deformations of four ballast materials having different gradations and aggregate shape properties. An imaging device was used to create accurate particle size distributions and shapes for measuring and quantifying by indexes the ballast aggregate shape properties, that is, particle flatness and elongation and angularity. On the basis of the results of the DEM modeling study, a bridge approach settlement ramp was constructed and tested at the Transportation Technology Center's Facility for Accelerated Service Testing. The results showed that the settlement ramp approach could be achieved by constructing ballasted track with proper selection of materials in each section of track transition zone. This study also demonstrated that the DEM simulation approach combined with image analysis could be used as a quantitative tool for predicting the ballast performance and providing help in design of track transitions.

Bridge approaches and low-modulus track transition zones create significant settlements and cross-level and alignment problems. In these locations, a shift from open deck to ballasted deck superstructures has been somewhat effective for mitigating these problems, because of the use of the same fastening system and tie design and spacing from bridges to approaches, but skewed abutments still often cause differential (cross-level) tie support problems. Approximately $200 million is needed every year just to maintain track transitions (*1, 2*). For ballasted deck concrete or steel bridges with concrete ties, reducing stiffness and increasing track damping on the bridge can effectively reduce impact forces and degradation of track components and track geometry. Kerr and Bathurst focused on reducing track stiffness on the bridge by using special pads and ties (*3*). This had some mitigating effect on the transition problem by decreasing the stiffness difference between the bridge and the approach, but differential settlement was still developing between the bridge and the approach embankment, especially where settlement was caused by geotechnical problems (*4*). Li and Davis identified inadequate ballast and subballast layer performance as the primary cause of track geometry degradation (*4*). In addition, Davis et al. listed the factors most significant to bridge approach transitions as subgrade and ballast condition, ballast thickness, crosstie type, and wheel load (*5*). Similarly, Davis and Chrismer used track settlement and vertical deflection data from a bridge of a western railroad to suggest that the ballast layer was the major source of railway transition settlement (*6*). Recently, Mishra et al. conducted field settlement measurements by using multidepth deflectometers in three problematic bridge approaches near Chester, Pennsylvania, and concluded that the ballast layer was the primary source contributing to recurring differential settlements and track geometry problems (*7*).

With the objective of providing better engineering insight into the design of ballasted track for improving railroad safety and network reliability, recent research at the University of Illinois has developed a ballast performance model based on the discrete element method (DEM) that uses rigid but randomly shaped three-dimensional polyhedrons or blocks as the basic elements for realistically simulating interactions, such as movement and interlock, of contacting ballast aggregate particles. The ballast DEM model requires as input imaging-based aggregate size and shape quantifications. Among the various particle shape and morphological indexes, the flat and elongated (F&E) ratio, the angularity index (AI), and the surface texture (ST) index—all developed with the University of Illinois aggregate image analyzer (UIAIA)—are key indices, described in detail elsewhere (*8, 9*). The UIAIA system takes images of an individual aggregate particle from three orthogonal views to quantify imaging-based F&E ratio and ST morphological indices and the AI. The image-aided DEM approach then uses the UIAIA scanned images to recreate the three-dimensional aggregate shapes as individual discrete elements.

The ballast DEM model was calibrated in earlier research efforts with laboratory direct shear (shear box) ballast strength test results and then used to model strength and settlement behavior of railroad ballast for studying the effects of multiscale aggregate morphological properties and ballast fouling influencing track performance

Y. Qian, E. Tutumluer, Y. M. A. Hashash, and J. Ghaboussi, Department of Civil and Environmental Engineering, University of Illinois at Urbana–Champaign, 205 North Mathews Avenue, Urbana, IL 61801. D. D. Davis, Transportation Technology Center, Inc., 55500 DOT Road, Pueblo, CO 81001. Corresponding author: E. Tutumluer, tutumlue@illinois.edu.

Transportation Research Record: Journal of the Transportation Research Board, No. 2476, Transportation Research Board, Washington, D.C., 2015, pp. 45–52.
DOI: 10.3141/2476-07

(*10–13*). For the field application of the DEM model, ballast settlement data were collected from the Facility for Accelerated Service Testing (FAST) for heavy axle load applications at the Transportation Technology Center (TTC) in Pueblo, Colorado. Four 100-ft test sections were constructed in early 2010 with four different aggregate materials used as the new ballast layer installations on a curve at the TTC FAST test track. Preliminary results from the dynamic, repeated train loading simulations indicated that the ballast DEM model could predict magnitudes of the field ballast settlements from both early loading cycles and over 100 million gross tons (MGT) performance trends reasonably accurately. Hence the ballast settlement predictions are sensitive to both aggregate shape and gradation (*14*).

This paper presents the development of an innovative method for designing a bridge approach settlement ramp and for mitigating differential settlement in engineered ballast zones. Grain size distributions and particle shape properties were collected from 13 ballast materials. Four ballast materials were selected for building a settlement ramp according to previous findings from field testing and DEM numerical simulations (*14*). Full-scale track DEM simulations were performed for selecting the materials placed in the engineered ballast zones. Finally, field testing was conducted to collect data on the performance of the bridge approach settlement ramp, compare those materials with the DEM simulation results, and validate the design concept.

OBJECTIVE AND SCOPE

The overall objective of this paper is to introduce an innovative approach to transition zone design for mitigating ballast differential settlement through selection of appropriate ballast materials and placing them in appropriate zones, that is, the settlement ramp. A full-scale railroad ballast model based on the DEM and aggregate image analysis were successfully adopted for realistically predicting trends in ballast permanent deformation. The study scope included evaluating size and shape properties of 13 ballast materials collected from different suppliers, all approved for track use under typical dynamic train loads induced by heavy-axle-load freight cars in North America. Field testing at the TTC was undertaken through the construction of a bridge approach transition zone with various ballast materials placed in an orderly fashion in the track settlement ramp, according to ballast settlement amounts predicted by the DEM simulations. This innovative approach, which integrates the DEM simulation platform with imaging-quantified particle shape properties, can be applied to locations where most differential settlement occurs within the ballast layer, allowing design and engineering of the ballast settlement in a more uniform transition.

TRACK TRANSITION ZONE DESIGN

Settlement Ramp Concept

Tutumluer et al. performed full-scale track simulations with imaging-quantified ballast particle shape properties and the developed DEM model to study ballast settlement behavior and validate the modeling approach through field testing (*14*). The ballast settlement data predicted by the DEM simulations clearly showed that more cubical particles with higher AI yielded higher settlement compared with more rounded particles having lower AI values. A ballast settlement ramp concept based on the hypothetical relationship between particle shape properties in micro scale and ballast settlement in macro scale adopted by Tutumluer et al. was proposed to mitigate the effects of the bridge approach differential settlement, that is, the bump at the end of the bridge (*14*). It was proposed that the settlement ramp be constructed with various properly selected ballast materials to produce gradually changing ballast settlement amounts, so that the overall differential settlement at the bridge approach would be reduced. Through ramping settlement, the bump at the abutment caused by the significantly higher differential settlement was made into a ramp so that differential settlements would gradually increase for exiting the bridge deck or would reduce for entering the bridge to allow required maintenance and improve safety and ride quality. However, the following field limitations had to be considered for the proposed settlement ramp design: (*a*) field test sections would be constructed with available ballast materials (no custom gradations or particles) and (*b*) field test sections could not be longer than 24 m (80 ft) in total. With these field limitations, a bridge approach prototype was developed to use four ballast sections or zones 6 m (20 ft) long. Ballast Zone 4 (BZ 4), starting 24 m from the bridge, was intended to have the highest settlement rate. Moving toward the bridge, each subsequent zone was intended to have lower settlement rates. Additionally, the ballast on the bridge was selected to match the settlement rate of the ballast closest to the bridge. Figure 1 presents the design concept for the transition zone settlement ramp.

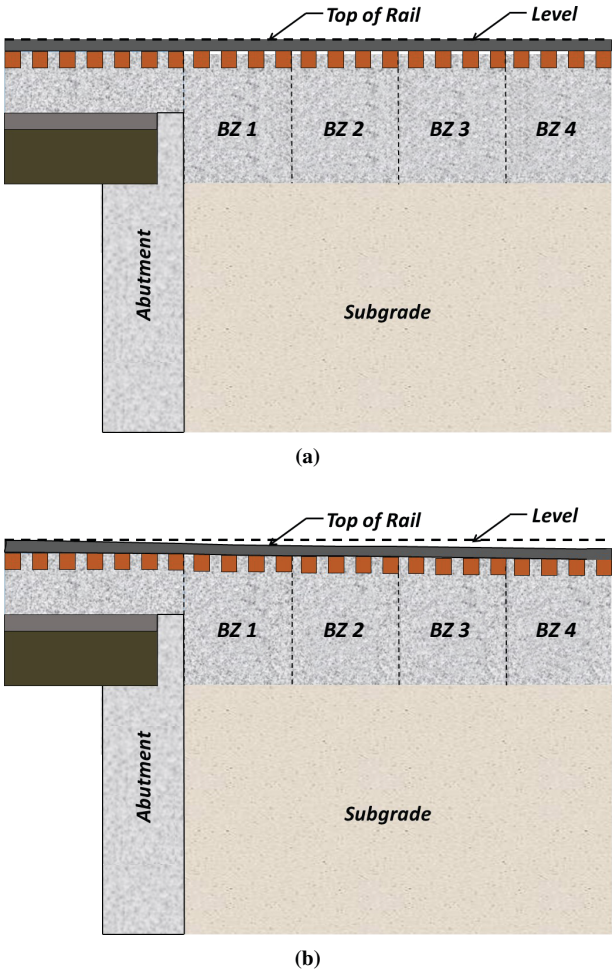

FIGURE 1 Design concept for track transition zone settlement ramp: (*a*) before loading and (*b*) after loading.

Ballast Material Properties and Image Analysis

Thirteen ballast materials donated by a major Class I railway company and from various suppliers in North America were received in the laboratory. All 13 ballast materials were processed for collecting necessary modeling information, such as grain size distribution and shape properties. Shape properties of the ballast particles, such as AI, F&E ratio, and ST index, were analyzed with the UIAIA (*8, 9*). The gradations and particle shape indexes quantified from the UIAIA were needed later on to generate individual particles, referred to here as elements, used in DEM simulations (*14*). The sieve analysis and image analysis results are summarized and presented in Figure 2 and Table 1, respectively. Also listed in Table 1 are the coefficient of uniformity (C_u) and the coefficient of curvature (C_c) of the 13 ballast materials.

TABLE 1 Properties and UIAIA-Based Shape Indexes of Studied Ballast Materials

Ballast Type	AI Index	F&E Ratio	ST Index	C_u	C_c
Material 1	468	2.4	2.7	1.58	1.01
Material 2	537	2.0	1.4	1.71	1.03
Material 3	433	1.8	1.1	1.59	1.01
Material 4	411	2.0	1.0	1.85	0.96
Material 5	378	1.9	1.1	1.72	1.03
Material 6	414	1.8	1.8	1.59	1.02
Material 7	426	2.0	1.6	2.38	1.04
Material 8	488	2.0	1.1	1.65	1.01
Material 9	387	1.9	0.9	1.70	1.08
Material 10	440	2.3	2.0	1.46	0.97
Material 11	601	2.0	3.1	1.44	1.09
Material 12	411	2.0	0.9	1.79	1.02
Material 13	590	3.5	2.5	2.25	1.14

Selected Ballast Materials for Settlement Ramp

According to the grain size distributions and imaging-based particle shape indexes and the settlement performances of the field test sections studied recently by Tutumluer et al. (*14*), ballast materials 5, 7, 11, and 13 were selected for constructing the four ballast zones BZ 1, BZ 2, BZ 3, and BZ 4, respectively. Table 2 lists each selected ballast material and its suggested construction zone in the settlement ramp. Ballast material 5 was selected for use in BZ 1 because it had the lowest AI (more rounded) and hence gave the least amount of settlement from the DEM simulation results of all the four ballast sections. Materials 11 and 13 were selected for relatively higher settlement potentials because both materials had higher imaging-based AI. Although the AI values of ballast materials 11 and 13 were similar, material 13 had particles with higher F&E ratios than material 11. Particles with higher F&E ratios were more likely to break in track (*14*); hence material 13 was selected for BZ 4 for the highest settlement potential, and material 11 was selected for use in BZ 3 for the second-highest settlement potential. Material 7 was estimated to yield settlement amounts less than ballast material 11 but more than material 5. Accordingly, ballast material 13 was chosen as the baseline ballast. It was assumed that BZ 4 was used on the line segment for which the bridge approach was designed. Thus, the same ballast was used on the ballasted bridge deck.

DISCRETE ELEMENT MODELING

With the UIAIA imaging-based shape indexes listed in Table 1 and grain size distributions given in Figure 2, the DEM simulation platform developed at the University of Illinois was used to conduct numerical simulations of ballast settlement behavior using the actual field geometry and train loading characteristics of the TTC FAST conditions. Figure 3 shows a full-scale track DEM simulation

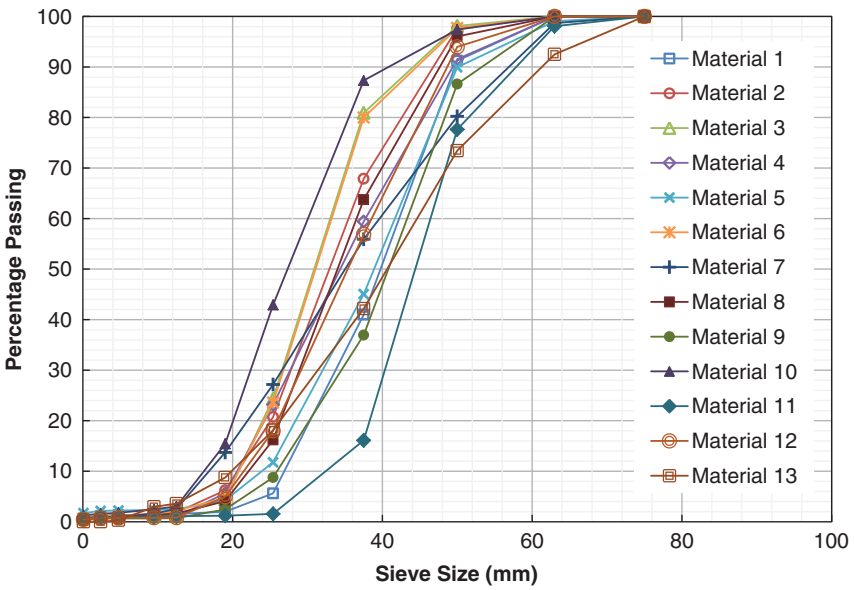

FIGURE 2 Grain size distributions of studied ballast materials.

TABLE 2 Ballast Materials Selected for Construction

Ballast Zone	Ballast Type	Remarks
BZ 1	Material 5	Lowest AI (378 degrees)
BZ 2	Material 7	Highest C_u (2.38)
BZ 3	Material 11	Highest AI (601)
BZ 4	Material 13	Highest F&E (3.5), high C_u (2.25)

model, which contains about 13,000 particles under one tie supported by half the tie spacings on either side of the loaded tie. The thickness of the ballast layer is about 0.305 m (12 in.) and the tie spacing is 0.61 m (24 in.). Boundaries are set perpendicular to the longitudinal direction of track and at the bottom of the ballast layer. There is no boundary to restrain particle movement in the lateral direction of the track. Discrete elements representing ballast particles in simulations are not allowed to cross the boundaries, and the contacts between the boundaries and particles are the same as contacts between different particles. The load pulse applied in the simulation was modified according to a dynamic track model (*15*) to simulate 39-ton axle loading at a speed of 64 km/h (40 mph). Details of the load pulse and the discretely supported track model are available elsewhere (*14*). The initial ballast densities used in the DEM simulations were calculated according to laboratory compaction testing with a metal box. Materials 5, 7, and 11 were compacted with a roller compactor in the same metal box used in a previous study, which had established the initial density of field compacted material 13 (*14*). Accordingly, the initial densities of the ballast materials estimated for use in the DEM simulations are listed in Table 3. Table 4 lists the modeling parameters used in the DEM simulations.

Because of the high computational resources required for the DEM model simulations, the number of dynamic load pulses from individual freight cars to be applied cannot be as high as in the actual field loading conditions—for example, hundreds of thousands of car passes corresponding to tens of thousands of MGT. Previous field validation showed that the long-term field performance could be estimated from relatively few simulation traffic passes with reasonable accuracy (*14*). Figure 4 presents the computed settlement values from the DEM simulations undertaken up to 1,000 car passes. By adequately addressing the ballast grain size distributions, imaging-based particle shape characteristics as well as initial ballast conditions, the DEM simulations computed the settlement trends of the four ballast zones as shown in Figure 4. The predicted amounts of ballast settlement for the various ballast zones followed the order

TABLE 3 Initial Density of Each Ballast Material Used in DEM Simulations

Ballast Zone	Ballast Type	Porosity (%)
BZ 1	Material 5	32
BZ 2	Material 7	33
BZ 3	Material 11	38
BZ 4	Material 13	32

TABLE 4 Modeling Parameters Used in DEM Simulations

Description	Value
Interparticle friction angle	31°
Normal contact stiffness	20 MN/m
Shear contact stiffness	10 MN/m
Global damping	0
Contact damping	0.4

BZ 3, BZ 4, BZ 2, and BZ 1 from high to low. All the particles in simulation were considered as rigid and nonbreakable elements. However, in previous field testing it was noticed that material 13 yielded higher settlement in the field than the value predicted by DEM simulation (*14*). Thus, the DEM simulation results confirmed the materials selection for construction of each section in the field testing. All the ballast materials evaluated in this study were crushed aggregates. Ballast materials should be crushed to have certain angularity to ensure shear strength and stability of the track. However, if the angularity of particles is too high, good packing with the least amount of voids in the assembly may be difficult to achieve until adequate particle shakedown with slow trains. With crushed and cubical particles and good stabilization and compaction in the field, ballast can have low settlement potential and high angularity to ensure strength and track stability.

FIELD TESTING AND VALIDATION

Field Testing Conditions

With the four selected ballast materials, the proposed settlement ramp consisting of the four ballast zones (BZ 1, BZ 2, BZ 3, and BZ 4) was built on a 5° curve at the TTC FAST high tonnage loop (Figure 5). The total length of the settlement ramp was 24 m, and each zone

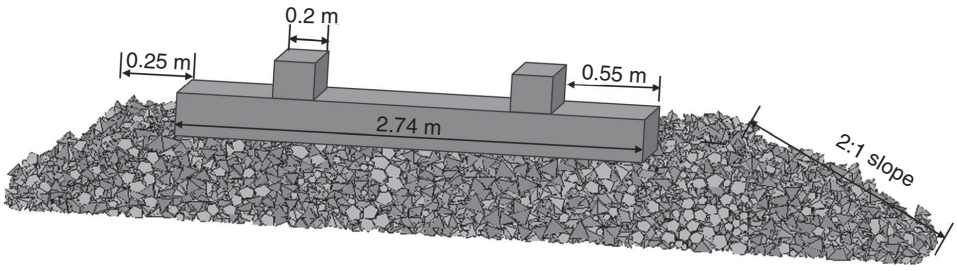

FIGURE 3 Full-scale track DEM simulation model.

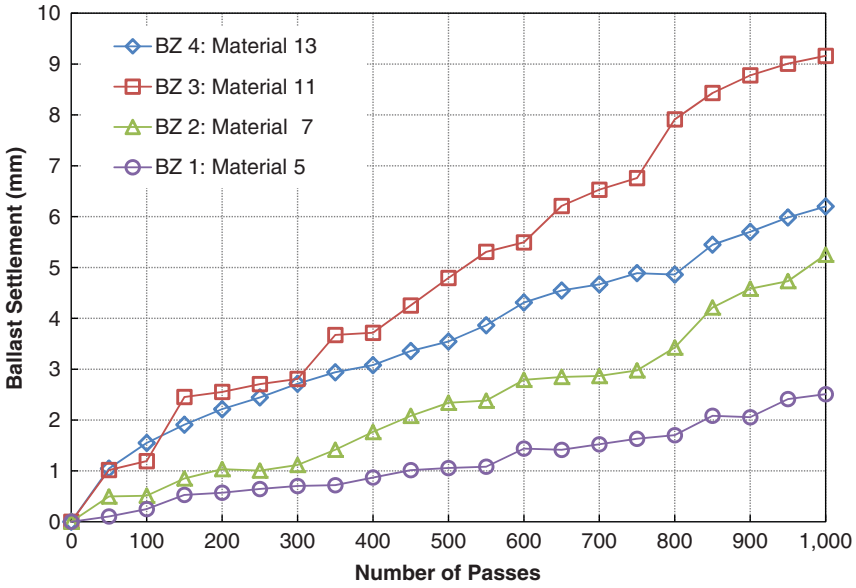

FIGURE 4 DEM simulation computed ballast settlement values.

was 6 m (20 ft). Figure 6 shows the field construction site. The field testing was conducted by a remote-controlled train that had 90 to 110 cars with 39-ton axle load operating at 64 km/h. In the initial loading stages, a 10-car train was used to monitor the performance. In the end, a total traffic of 100 MGT accumulated in the test track.

Field Testing Results

Figure 7 shows the average ballast settlement of each ballast zone or test section obtained from a settlement plate installed in that test section. The settlement plates were installed at the interface between subgrade and ballast in each ballast zone. A telltale bar extending over the ballast was connected to the plate to indicate the settlement of the subgrade. The ballast settlement in each zone could then be calculated according to the survey data of the subgrade settlement subtracted from the total top of rail settlement. The same general pattern of settlement was observed in each test section. There was a high initial settlement, ranging from 20 to 50 mm, depending on the ballast materials for the initial stage of loading for up to about 6 MGT. Then, a certain amount of track rebound happened during ballast shift, that is, particle flow and particle breakage, under dynamic train load. Also, loss of superelevation was observed, which caused the low rail to rise. A broken rail was detected in BZ 3 when the loadings were accumulated to 15 MGT. The repair of the broken rail and resurfacing of the track after the repair may have contributed to the rebound, as indicated in Figure 7.

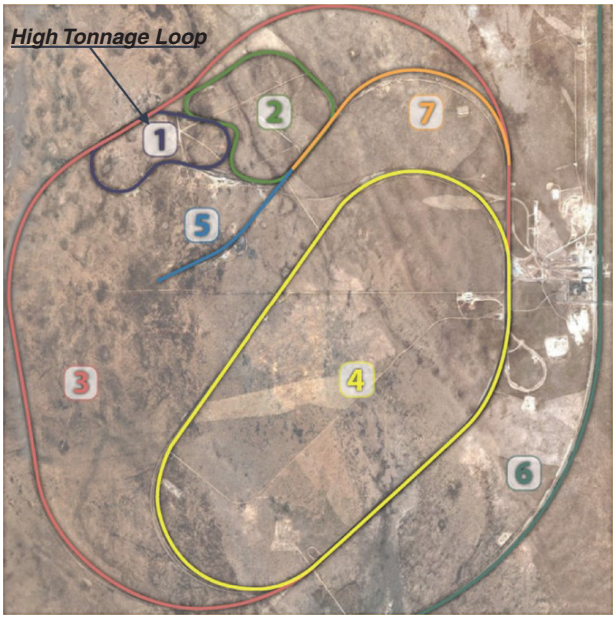

FIGURE 5 FAST high tonnage loop at TTC in Pueblo, Colorado. (Source: TTC.)

The initial high settlements shown in Figure 7 were most likely caused by an initial shakedown of the newly constructed ballast test sections. Later on, settlement in each section further increased at a relatively steady rate of between 15 and 36 MGT. After 36 MGT, the test track was surfaced again, which caused settlements to accumulate at a noticeably higher rate. The next settlement measurement was taken at 64 MGT, when the plate measurements showed the settlements were controlled by a decreasing rate and the track reached a consolidated steady state.

The settlement trends predicted by the DEM model generally matched the performance of the field test sections. The field settlement trends followed the order Bridge < BZ 1 < BZ 2 < BZ 3. The largest discrepancy was for the BZ 4 section, which was designed to have the highest settlement according to the DEM simulations. However, during the field validations with the BZ 4 section original ballast material [i.e., the study by Tutumluer et al. (*14*)], this ballast material had settlement amounts higher than that of the BZ 1 section ballast but lower than that of the BZ 2 section ballast. The supplier of the BZ 4 section ballast material had changed crusher type in the plant, and hence the ballast sample that was collected and tested in the laboratory had shape properties that were different from those of

(a) (b) (c)

FIGURE 6 Construction photos of TTC FAST bridge site.

the ballast material constructed in the bridge approach test zone. This difference is the reason the measured settlement of BZ 4 is denoted as BZ 4: Material X in Figure 7. It is likely that the ballast material (Material X) used for construction of BZ 4 had fewer F&E particles than the sample used to make predictions based on the laboratory imaging tests. Accordingly, except for the BZ 4 test section farthest from the bridge abutment, the settlement ramp design was successfully accomplished.

The material used in section BZ 4 was also used on the ballasted bridge deck. Hence, any difference in settlement between the bridge deck and the BZ 4 sections is linked to the effects of the rigid bridge foundation on the ballast permanent deformation. The lack of subgrade and lateral confinement of the ballast in the bridge deck ballast pan caused a reduction in the settlement rate. However, the difference in settlement of the bridge deck and the BZ 1 section is the differential settlement that can be observed at the end of the ballast deck bridge. It is clear that selecting the appropriate ballast material to construct the test zones of a settlement ramp for anticipated performance trends, in this case BZ 1, BZ 2, and BZ 3, could effectively reduce differential settlement immediately near the bridge abutment to some degree.

The track stiffness of each test section was also measured during the field performance testing. It was expected that track stiffness would increase from the approach toward the bridge, and the field test sections before trafficking did behave in this manner. The bar charts in Figure 8 compare the track stiffness values measured at the center of each test section. The measurements after 12 MGT showed a decline in track stiffness from the initial values, which may be related to the broken rail replacement. However, the average track stiffness after 12 MGT in general increased as the accumulation of tonnage increased.

Lateral track stiffness represents the ability of a ballast section to hold track alignment. Single tie push tests were performed to assess the lateral track stiffness right after construction with no traffic loading and after 112 MGT. Figure 9 presents the results of the single tie push test in each ballast section. Lateral track stiffness of the ballast

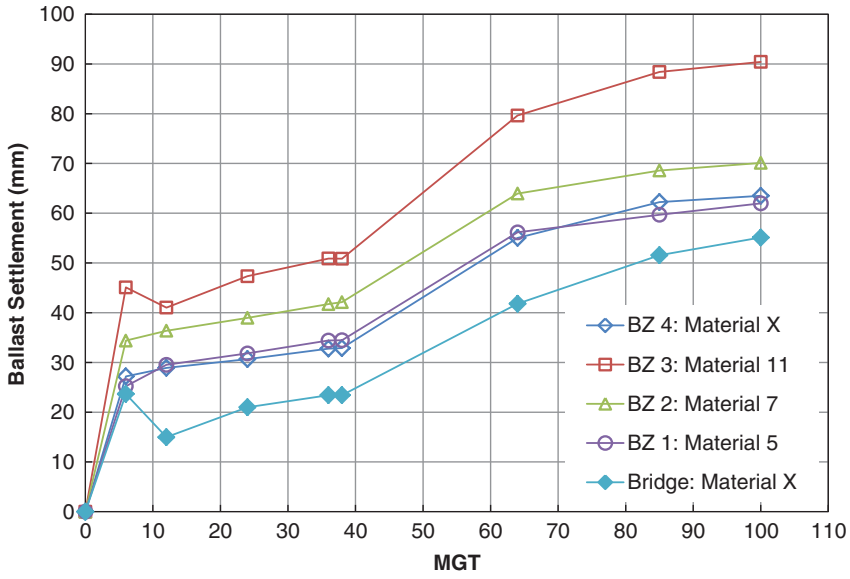

FIGURE 7 Average track settlements graphed with traffic for each ballast test section.

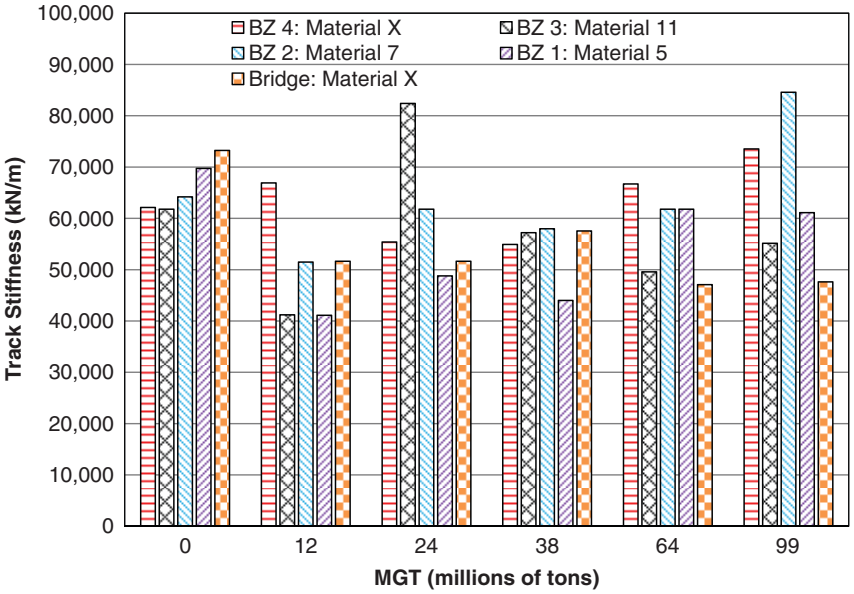

FIGURE 8 Track stiffness values measured with traffic for each ballast test section.

on the bridge deck was not measured because of logistical issues. As intended, the ballast section closer to the bridge had higher lateral stiffness. With accumulation of tonnage, ballast materials consolidated, which led to the increase in lateral stiffness. Three sections—BZ 1, BZ 2, and BZ 3—increased by about 30% in lateral stiffness, and BZ 4 increased by 350%.

CONCLUDING REMARKS

Ballast behavior not only depends on grain size distribution but also depends on particle shape properties. Ballast materials having similar grain size distributions, for example, satisfying certain American Railway Engineering and Maintenance-of-Way Association gradations, can have significantly different field performance characteristics, such as particle packing, settlement, and stiffness, if their particles have different shape properties. Such shape properties—flatness, elongation, angularity—have been successfully quantified through indexes based on image analysis to create similarly shaped individual three-dimensional particles for conducting realistic simulations of ballast behavior based on the DEM.

This paper presented an innovative approach to mitigating ballast differential settlement through selecting appropriate ballast materials according to their grain size and shape characteristics and placing them at various distances from a bridge abutment to build a settlement ramp in track transition zones. A full-scale ballasted track

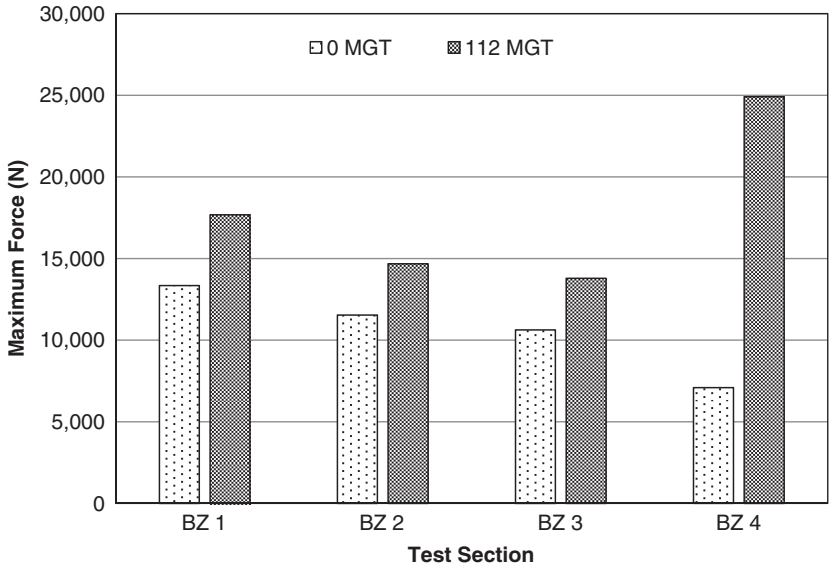

FIGURE 9 Single tie push test results for each ballast test section.

numerical model, developed with the DEM, was used to simulate settlement behavior of the ballast materials used in each section of the designed settlement ramp. According to the results of the DEM modeling study, field construction and testing were undertaken at the FAST high tonnage loop at TTC in Pueblo, Colorado. Field testing results validated the design concept and the DEM simulation findings. A settlement ramp constructed with four different ballast materials was found to effectively reduce or mitigate differential settlement and provide a more uniform transition from open track to track on a structure, such as a bridge.

The DEM simulation platform developed at the University of Illinois could model full-scale track and corresponding heavy axle dynamic loading to capture ballast settlement behavior of various ballast materials by adequately addressing their detailed grain size distribution and particle shape properties. The DEM simulation platform, which is being further developed, has potential as a quantitative tool for predicting the ballast field performance and aiding track design.

ACKNOWLEDGMENTS

This research project was supported in part by the Association of American Railroads. Mike Wnek and Maziar Moaveni of the University of Illinois provided help with laboratory sieving and image analyses.

REFERENCES

1. Sasaoka, C., D. D. Davis, K. Koch, R. Reiff, and W. GeMeiner. *Technology Digest TD-05-001: Implementing Track Transition Solutions.* Transportation Technology Center, Inc., Pueblo, Colo., 2005.
2. Hyslip, J., D. Li, and C. McDaniel. Railway Bridge Transition Case Study. *Proc., 8th International Conference on Bearing Capacity of Roads, Railways, and Airfields,* Champaign, Ill., 2009.
3. Kerr, A., and L. Bathurst. *Upgrading Track Transitions for High-Speed Service.* DOT/FRA/RDV-02/05. FRA, U.S. Department of Transportation, 2001.
4. Li, D., and D. D. Davis. Transition of Railroad Bridge Approaches. *Journal of Geotechnical Engineering,* Vol. 131, No. 11, 2005, pp. 1392–1398.
5. Davis, D. D., R. Anaya, S. M. Chrismer, and L. Smith. *Technology Digest TD-07-002: Development of a Differential Settlement Model for Design and Maintenance of Track Transitions.* Transportation Technology Center, Inc., Pueblo, Colo., 2007.
6. Davis, D. D., and S. M. Chrismer. Track Differential Settlement Model. *Proc., ASME/IEEE Joint Rail Conference and Internal Combustion Engine Spring Technical Conference,* Pueblo, Colo., 2007.
7. Mishra, D., E. Tutumluer, H. Boler, J. P. Hyslip, and T. R. Sussmann. Railroad Track Transitions With Multidepth Deflectometers and Strain Gauges. In *Transportation Research Record: Journal of the Transportation Research Board, No. 2448,* Transportation Research Board of the National Academies, Washington, D.C., 2014, pp. 105–114.
8. Rao, C., E. Tutumluer, and I. T. Kim. Quantification of Coarse Aggregate Angularity Based on Image Analysis. In *Transportation Research Record: Journal of the Transportation Research Board, No. 1787,* Transportation Research Board of the National Academies, Washington, D.C., 2002, pp. 117–124.
9. Pan, T., E. Tutumluer, and J. Anochie-Boateng. Aggregate Morphology Affecting Resilient Behavior of Unbound Granular Materials. In *Transportation Research Record: Journal of the Transportation Research Board, No. 1952,* Transportation Research Board of the National Academies, Washington, D.C., 2006, pp. 12–20.
10. Tutumluer, E., H. Huang, Y. M. A. Hashash, and J. Ghaboussi. Aggregate Shape Effects on Ballast Tamping and Railroad Track Lateral Stability. *Proc., AREMA Annual Conference,* Louisville, Ky., 2006.
11. Tutumluer, E., H. Huang, Y. M. A. Hashash, and J. Ghaboussi. Discrete Element Modeling of Railroad Ballast Settlement. *Proc., AREMA Annual Conference,* Chicago, Ill., 2007.
12. Tutumluer, E., H. Huang, Y. M. A. Hashash, and J. Ghaboussi. AREMA Gradations Affecting Ballast Performance Using Discrete Element Modeling (DEM) Approach. *Proc., AREMA Annual Conference,* Chicago, Ill., 2009.
13. Qian, Y., S. J. Lee, E. Tutumluer, Y. M. A. Hashash, D. Mishra, and J. Ghaboussi. Discrete Element Method for Simulating Ballast Shear Strength from Large Scale Triaxial Tests. In *Transportation Research Record: Journal of the Transportation Research Board, No. 2374,* Transportation Research Board of the National Academies, Washington, D.C., 2013, pp. 126–135.
14. Tutumluer, E., Y. Qian, Y. M. A. Hashash, J. Ghaboussi, and D. D. Davis. Discrete Element Modeling of Ballasted Track Deformation Behavior. *International Journal of Rail Transportation,* Vol. 1, No. 1–2, 2012, pp. 57–73.
15. Huang, H., S. Shen, and E. Tutumluer. Sandwich Model to Evaluate Railroad Asphalt Trackbed Performance Under Moving Load. In *Transportation Research Record: Journal of the Transportation Research Board, No. 2117,* Transportation Research Board of the National Academies, Washington, D.C., 2009, pp. 57–65.

The opinions expressed in this article are those of the authors and do not represent the opinions of the funding agency.

The Standing Committee on Railway Maintenance peer-reviewed this paper.